PROTON RESONANCE STUDY OF THE WATER OF HYDRATION IN NATROLITE

PROTON RESONANCE STUDY OF THE WATER OF HYDRATION IN NATROLITE

By

GEORGE PAUL CANT, B.Sc.

A Thesis

Submitted to the Faculty of Graduate Studies

in Partial Fulfilment of the Requirements

for the Degree

Master of Science

McMaster University

January 1963

MASTER OF SCIENCE (1963) McMASTER UNIVERSITY
(Physics) Hamilton, Ontario.

TITLE: Proton Resonance Study of the Water of Hydration in Natrolite.

AUTHOR: George Paul Cant, B.Sc. (McMaster University)

SUPERVISOR: Professor H. E. Petch

NUMBER OF PAGES: vi, 50

SCOPE AND CONTENTS:

The nuclear magnetic resonance spectrum of the protons in the water of hydration in a single crystal of natrolite has been investigated and analysed according to Pake's theory in order to locate the protons in the structure.

The line shape of the proton resonance in natrolite powder was studied over a wide range of temperature. The observed changes in the line shape partially revealed the dynamics of the water of hydration.

ACKNOWLEDGEMENTS

I would like to thank Professor H. E. Petch for his suggestion as to the topic of this thesis, for the guidance which he offered me during the course of the experimental work, and for his constant interest in its progress. I am also grateful to J. D. Cuthbert for the countless valuable discussions with him concerning both theoretical and experimental aspects of this work.

The author received financial aid from McMaster University in the form of an assistantship. This research was supported by Defence Research Board of Canada grants-in-aid to Professor Petch.

TABLE OF CONTENTS

LIST OF ILLUSTRATIONS

LIST OF TABLES

INTRODUCTION

Nuclear magnetic resonance at ordinary radio frequencies was first introduced by Rabi, Millman, Kusch, and Zacharias in conjunction with their atomic beam experiments. Purcell, Torrey, and Pound (1946) and Bloch, Hansen, and Packard (1946) independently obtained the first magnetic resonance in bulk matter. Since then, many applications have been developed. Nuclear properties such as the gyromagnetic ratio and nuclear spins and dipole moments can be measured with very high accuracy owing to modern methods of measuring radio frequencies. Magnetic field strengths can be measured with an accuracy never before available and can be very precisely controlled. Following Pake's application (Pake 1948) of proton magnetic resonance to determine the location of the hydrogen atoms in the structure of gypsum there rapidly blossomed a wide field where magnetic resonance was developed as a probe to study molecular chemistry and the structures, interactions, and motions to be found in solids. A number of excellent pieces of theory are now available which allow us to determine from some of the resonance patterns observed certain configurations of atoms such as pairs, triangles, and tetrahedral arrangements and information regarding the dynamics of the atoms. However, only a start has been made. Ambiguities are still encountered in the interpretation of the spectra from many substances

and often the behaviour of the spectrum as the conditions of the specimen are altered simply defy explanation at this time. Fortunately, the theory concerning the interaction of two protons, as used in this work, is basic in the field of proton magnetic resonance and has been proven to be quite sound, especially in the many studies of hydrated crystals which have made use of Pake's theory.

CHAPTER I

Theory

I. 1. Introduction

This chapter summarizes the phenomenon of magnetic resonance and some of the theoretical calculations concerning the radio-frequency absorption spectra of two interacting, like spins in both single crystals and powdered solids.

When an atomic nucleus with spin I is placed in a magnetic field the observable component of the angular momentum is quantized such that only the values $m\hbar$, where $m = I, I-1, \ldots\ldots, -I$ are permissible. Many isotopes possess a nuclear magnetic dipole moment $\vec{\mu}$, which is collinear with the spin and is also quantized by a magnetic field. The permissible values of the observable component of the magnetic moment are $\mu_z = \gamma m\hbar$ where γ is the absolute nuclear gyromagnetic ratio. The energy of an isolated magnetic dipole $\vec{\mu}$ in a magnetic field $\vec{B}_o = (0, 0, B_z)$ is $-\vec{\mu}\cdot\vec{B}_o = -\mu_z B_o$ consequently, application of a magnetic field to a nucleus gives rise to 2I+1 Zeeman energy levels of energies $-\gamma m\hbar B_o$, uniformly spaced by an amount $-\gamma\hbar B_o$. Since the selection rule $\Delta m = \pm 1$ applies, all possible transitions have the energy $-\gamma\hbar B_o$ and frequency $\nu_o = \gamma B_o/2\pi$. This may also be considered as the Larmor frequency of the precession of the spin axis due to the

torque exerted by the applied field upon the nuclear dipole.

In a bulk sample transitions between the Zeeman levels are observed by applying to the nuclei an electromagnetic wave of the required frequency to induce transitions and by detecting the net absorption of energy from the source of excitation. Since the probability for both upward and downward transitions is the same, there must be a greater population of nuclei in the lower energy levels in order that a net absorption of energy occur. Upon initial application of the excitation, the Boltzmann population distribution provides a slight excess of nuclei in the lower Zeeman levels thus causing net energy absorption, and thereafter an equalizing of the populations of the levels is prevented by non-radiative spin-lattice relaxation mechanisms thus allowing a continuing but less pronounced absorption of energy, which eventually appears as heat in the bulk matter containing the resonating nuclei.

I. 2. Proton Magnetic Resonance

The proton has spin quantum number $I = \frac{1}{2}$ and therefore $m = \pm \frac{1}{2}$. The two Zeeman levels have a separation $\gamma \hbar B_o = 2\mu_z B_o$ where B_o is the magnetic flux density of the applied field. The entire spectrum consists of one line at 42.5760 B_o Mc./s. where B_o is given in wb./m.^{2}

In solids and liquids, however, interactions between the resonating nuclei and their neighbours cause a more complicated pattern of nuclear energy levels, investigation

of which leads to considerable knowledge of the nature of these interactions.

Consider a system composed of two protons separated by a short distance, such as one finds in water molecules. In addition to the applied field, B_o, each proton experiences the small magnetic field of the magnetic dipole moment of the other proton. Pake has treated this matter quantum-mechanically by considering the two protons as a system with total spin of 1 and three energy levels corresponding to m = +1, 0, and -1. The interaction between the proton dipoles perturbs these three levels as shown in Fig. 1. The separation between the levels produces two spectral lines at frequencies

$$\nu = \frac{2\mu_z B_o}{h} \pm \frac{3\mu_z^2 \mu_o}{hr^3 4\pi} (3 \cos^2\theta - 1) \quad \text{c./s.} \quad \ldots\ldots(1)$$

where μ_z = the proton moment, 1.41041×10^{-26} amp.-m.^{2}

r = the distance between the two protons, in meters

μ_o = the magnetic permeability of free space, $4\pi \times 10^{-7}$ kg.-m./coul.^{2}

h = Planck's constant, 6.62517×10^{-34} joule-sec.

B_o = the applied field, in wb./m.^{2}

θ = the angle between the externally applied magnetic field and the line joining the protons.

Figure 1

The three Zeeman energy levels of a two proton system. On the left is shown the level scheme when only the interaction with the applied field is considered. At the right is shown the perturbing effect of the magnetic dipole interaction between the protons. The energies are given beside each level. The allowed transitions and the appearance of the spectrum are also illustrated.

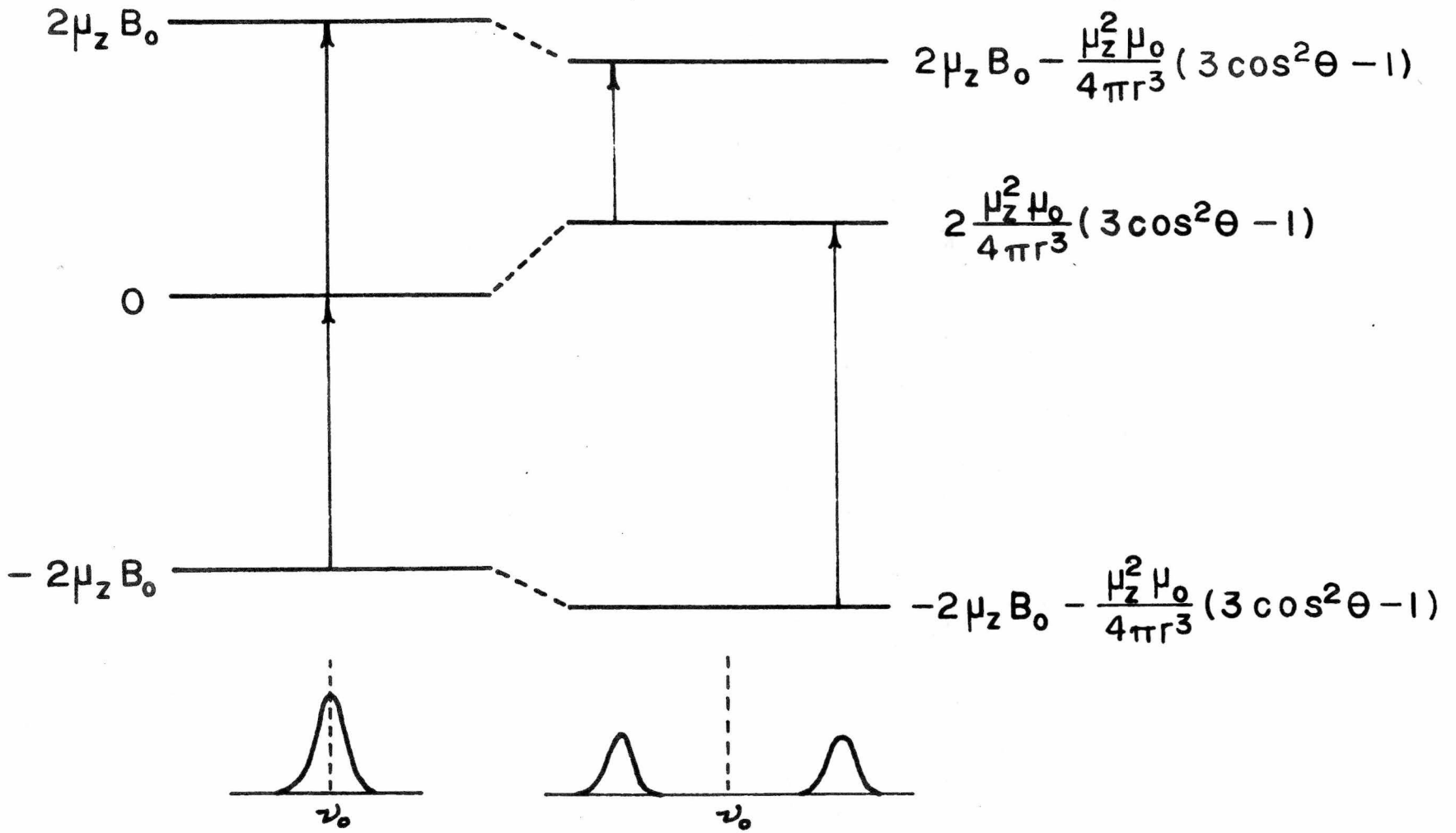
$2\mu_z B_0$
$2\mu_z B_0 - \frac{\mu_z^2 \mu_0}{4\pi r^3}(3\cos^2\theta - 1)$
$2\frac{\mu_z^2 \mu_0}{4\pi r^3}(3\cos^2\theta - 1)$
0
$-2\mu_z B_0$
$-2\mu_z B_0 - \frac{\mu_z^2 \mu_0}{4\pi r^3}(3\cos^2\theta - 1)$
ν_0
ν_0

The two signals are symmetrically placed on each side of the unperturbed proton frequency, ν_o, and their frequency separation is independent of the applied field.

Several factors cause each resonance line to have a width of several kc./s. The magnetic dipoles located within a few Angstroms of a nucleus participating in the resonance create small local fields of the order of 10^{-4}wb./m.^{2} superimposed on the applied field. The algebraic sum of these local fields depends on the orientations of the neighbouring dipoles. The vast number of combinations of orientations that are possible causes a continuous range of values of this local field. Therefore, at different times and places in the sample, resonating nuclei can be found in a variety of magnetic field strengths, and the observed absorption line appears as a gaussian curve. Any other source of variation of the field through the sample, such as inhomogeneity of the applied field, causes a further broadening of the lines.

In a typical investigation of a single crystal containing proton pairs, the crystal is mounted on a rotation axis which is maintained perpendicular to the applied field. The geometry for a crystal rotation is shown in Fig.2. θ denotes the angle between the field B_o and the line joining the protons P, hereinafter referred to as the p-p line. Φ is the angle between B_o and an arbitrary axis which is fixed relative to the crystal. Φ_o is the angle between the

Figure 2

A geometrical diagram to illustrate the angles and axes used in describing a single crystal rotation.

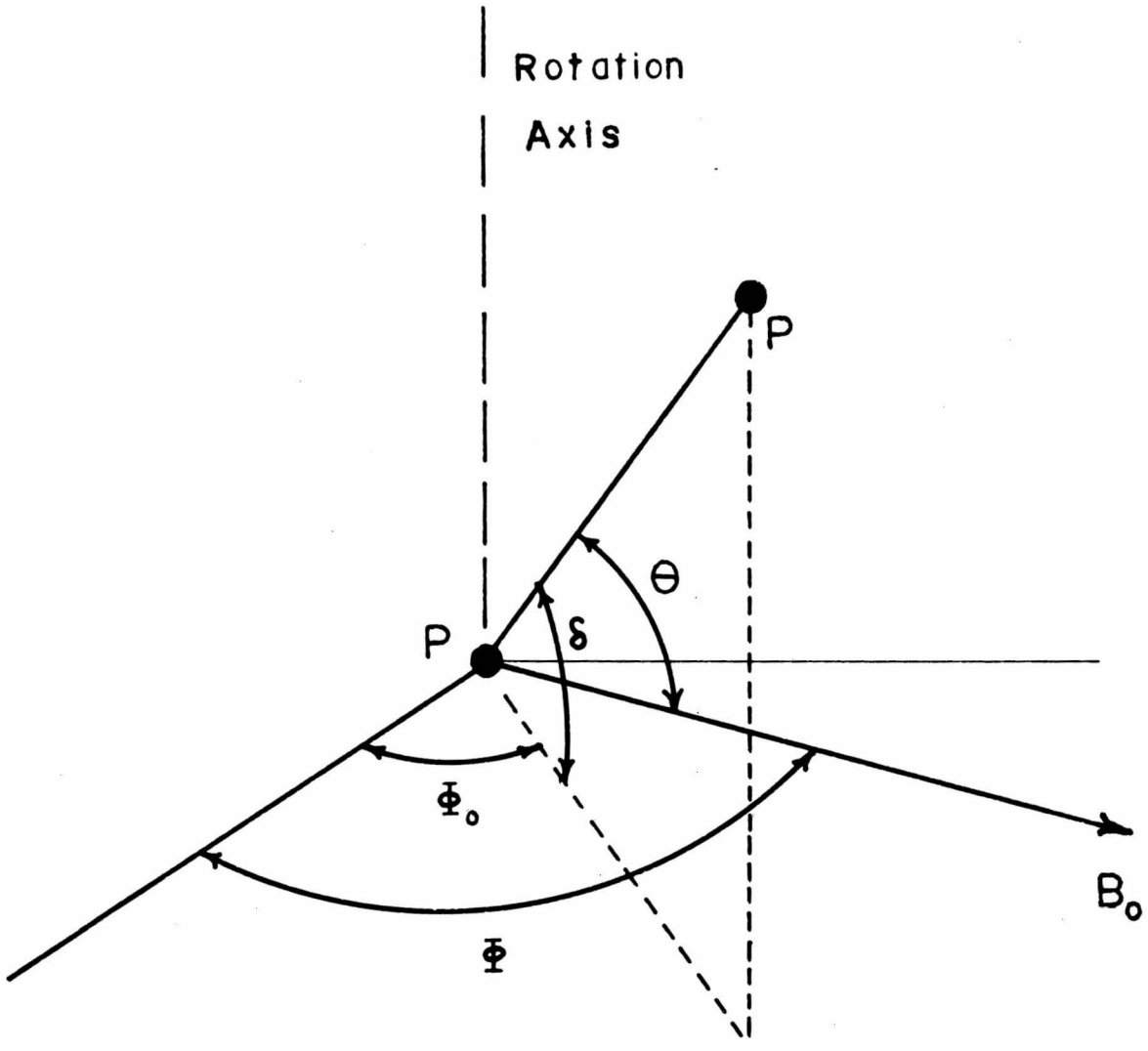
Rotation
Axis
P
P
θ
δ
Φ₀
Φ
B₀

aforementioned reference axis and the projection of the p-p line on the plane perpendicular to the rotation axis. δ is the angle between the p-p line and its projection on the plane perpendicular to the rotation axis. It can be seen that

$$\cos^2\theta = \cos^2\delta \cos^2(\Phi - \Phi_o)$$

The sinusoidal variation of signal separation ($\Delta\nu$) for a rotation of the crystal follows a "Pake Curve":-

$$\Delta\nu = \frac{3\mu_z^2}{2hr^3}\frac{\mu_o}{\pi}\left[3\cos^2\delta\cos^2(\Phi - \Phi_o) - 1\right] \quad .....(2)$$

From measurement of $\Delta\nu$ versus Φ the parameters δ, Φ_o, and r can be determined thereby giving the length of the p-p line and its direction with respect to the rotation axis and the reference axis.

Obviously if there is more than one p-p direction or length in the unit cell, a separate Pake curve with appropriate phase and amplitude is associated with each type of p-p line.

I. 3. Resonance Line Shape in a Powder

For a powder containing proton pairs the absorption curve, as expected, is the sum of the absorptions from each tiny single crystal in the sample. The following simple argument, assuming infinitely narrow resonances, shows how the powder spectrum is deduced. Firstly, the random orientation of the grains means that there is an

isotropic distribution of p-p directions. Thus the number of p-p lines whose angle with the field lies in the range θ to $\theta + d\theta$ is proportional to $\sin\theta\, d\theta$. Now the strength of the absorption between frequencies $\nu(\theta)$ and $\nu(\theta) + d\nu(\theta)$ is proportional to the number of p-p lines appropriately inclined to the field so as to give a line in that frequency range. Therefore $f(\nu)\, d\nu$ varies as $\sin\theta\, d\theta$ where $f(\nu)$ is the spectrum density. Evaluating $\sin\theta \frac{d\theta}{d\nu}$ in terms of ν and bearing in mind the frequency bounds within which the two signals from a proton pair are confined, one finds for the line shape:-

$$f(\nu) = \left(1 - \frac{(\nu-\nu_0)\, 4\pi hr^3}{3\mu_z^2\, \mu_0}\right)^{-\frac{1}{2}} \quad \text{for} \quad \frac{-3\mu_z^2\, \mu_0}{2\pi hr^3} < \nu - \nu_0 < \frac{-3\mu_z^2\, \mu_0}{4\pi hr^3}$$

$$f(\nu) = \left(1 - \frac{(\nu-\nu_0)\, 4\pi hr^3}{3\mu_z^2\, \mu_0}\right)^{-\frac{1}{2}} + \left(1 + \frac{(\nu-\nu_0)\, 4\pi hr^3}{3\mu_z^2\, \mu_0}\right)^{-\frac{1}{2}}$$

$$\text{for} \quad -\frac{3\mu_z^2\, \mu_0}{4\pi hr^3} < \nu - \nu_0 < \frac{3\mu_z^2\, \mu_0}{4\pi hr^3}$$

$$f(\nu) = \left(1 + \frac{(\nu-\nu_0)\, 4\pi hr^3}{3\mu_z^2\, \mu_0}\right)^{-\frac{1}{2}} \quad \text{for} \quad \frac{3\mu_z^2\, \mu_0}{4\pi hr^3} < \nu - \nu_0 < \frac{3\mu_z^2\, \mu_0}{2\pi hr^3}$$

This function is shown in Fig.3(a). When the dipolar broadening of the lines is taken into account an absorption

Figure 3

(a) Absorption curve for a powder containing proton pairs, assuming nearest neighbour interactions only.

(b) Absorption curve for a powder containing proton pairs, assuming the presence of interactions from all other neighbours. The corresponding derivative curve is also shown. (After Pake)

The frequency is indicated on the horizontal scale.

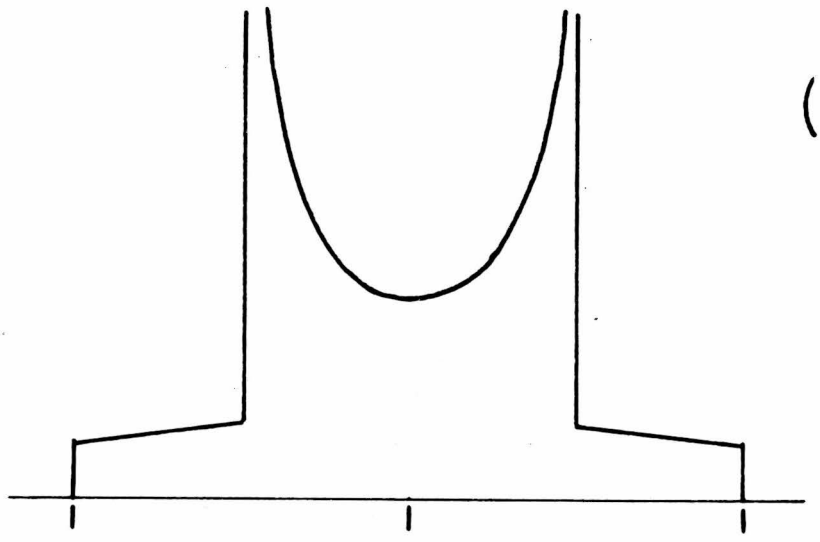

$$\nu_o - \frac{3\mu_z^2\mu_o}{2\pi h r^3} \qquad \nu_o \qquad \nu_o + \frac{3\mu_z^2\mu_o}{2\pi h r^3}$$

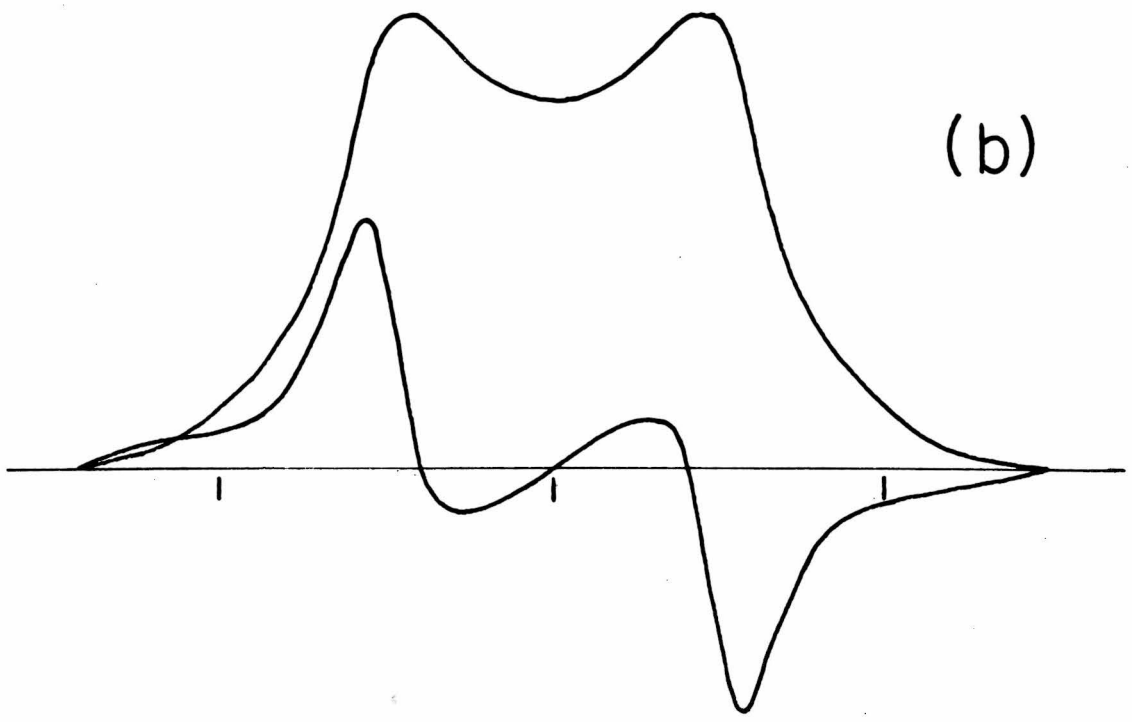

curve and derivative of the shape illustrated in Fig. 3(b) are obtained.

I. 4. Moments of a Resonance Curve

The line shape for two interacting spins is readily predicted, but the problem of three spins is considerably more complicated. As the number of strongly interacting spins is increased the task becomes so formidable that only very special cases of high symmetry can be treated. In any event, the line structure for five or more spins would generally be so complex that nothing could be resolved, especially with a powder sample. Fortunately, these difficulties do not render magnetic resonance useless as a means of ascertaining information about the arrangement of the atoms. Van Vleck (1948) has made theoretical calculations of the moments of the absorption intensity in terms of the position and strength of the various nuclear dipoles in the crystal structure. The n^{th} moment of a resonance curve is defined as

$$(\Delta\nu)^n = \int_0^\infty (\nu-\nu_0)^n f(\nu)\, d\nu$$

Where the dominant source of broadening in the line is magnetic dipolar interaction the resonance is symmetrical about ν_0 and the odd moments are equal to zero. Van Vleck's calculation of the second moment yields the following result,

where the resonance is obtained at fixed frequency by varying the applied field.

$$(\Delta B)^2 = \frac{3\mu_j^2\mu_o}{2N_s 4\pi} \sum_{j>k} \sum_{k} (3\cos^2\theta_{jk} - 1)^2 / r_{jk}^6$$

$$+ \frac{\mu_o}{3N_s 4\pi} \sum_{j} \sum_{f} \mu_f^2 (3\cos^2\theta_{jf} - 1)^2 / r_{jf}^6$$

where N_s = the number of interacting resonating nuclei

μ_j, μ_f = the absolute nuclear magnetic dipole moments of the resonant nucleus j and the non-resonant nucleus f, respectively.

θ_{jk}, θ_{jf} = the angles between the applied field and the lines joining the nucleus j with resonant nucleus k and non-resonant nucleus f, respectively.

r_{jk}, r_{jf} = the distances between nucleus j and nuclei k and f, respectively.

The second moment is seen to be composed of two terms,

one being the contribution from the interaction that the nuclei in resonance have with each other and the second taking into account the proximity of other elements or isotopes with strong local fields. The formula makes it apparent that procurement of a value of the second moment can, in spite of the lack of detail in the line, strongly suggest the configuration involved, especially when safe assumptions can be made about some of the bond lengths and directions.

The second moment for a powder sample is deduced from the above expression by replacing $(3 \cos^2\theta - 1)^2$ by its average over a sphere, which is 4/5. The expression for the fourth moment of a resonance line is rather long and is rarely used in analysis of experimental results.

I. 3. Motional Narrowing

Admittedly magnetic resonance does not match X-ray and neutron diffraction in its power to solve problems concerning rigid structures. On the other hand, it becomes most valuable in the investigation of the dynamics of the atoms and molecules. In fact, before magnetic resonance met widespread usage, the great extent of molecular motion that occurs in solids was only partially realized.

The onset of these motions with rising temperature is revealed through their drastic effects on the width and moments of the resonances from nuclei in the moving configuration. In most cases the motion causes the spectrum

to decrease in width. The reason for this is best seen in the formulae for second moments. If the reorientation of the molecule occurs at a high enough rate, the average must be taken of $(3 \cos^2\theta - 1)^2$ over all the values of θ. An interesting example is that of a system rotating about an axis fixed at an angle θ' with respect to the field. The angle θ_{jk} that the line between nuclei j and k makes with the applied field is now replaced by γ_{jk}, the angle that it makes with the axis of rotation, and a factor $\frac{1}{4} (3 \cos^2\theta' - 1)^2$ is inserted into each term of the summation. For a powder, $\frac{1}{4} (3 \cos^2\theta' - 1)^2$ is averaged to 1/5. In the special case where the internuclear vectors are perpendicular to the reorientation axis it is seen that the motion causes the second moment to be $\frac{1}{4}$ as great as for a rigid configuration. Measurement of linewidth is found to contain less information about motion in solids, but the actual shape has been theoretically predicted for simple cases such as a nuclear pair with a fixed rotation axis. High speed rotation of a system of two like spins about an axis perpendicular to the internuclear vector causes the resonance from a powder sample to decrease in width by $\frac{1}{2}$ while retaining the same shape. Last of all, mention must be made of a type of motion found in all liquids and in many solids. The resonating nuclei are located in atomic configurations which tumble about randomly oriented axes, thereby averaging

to zero the local fields originating within the rotating configuration or molecule, and which move in translational fashion relative to the surrounding nuclei, thereby averaging to zero the intermolecular dipolar interactions. Thus the resonances from a liquid are characteristically very narrow, to the extent that the true linewidth is masked by the field inhomogeneity in a conventional low-resolution spectrometer. It is concepts such as those outlined above that can account for many of the observed changes in the resonance shape as the sample is heated and the atoms are incited to move about.

A matter requiring discussion is the rate of reorientation necessary to cause motional narrowing. In a rigid lattice, nuclei are observed to be precessing over a range of frequencies of the order of the linewidth, $\delta\nu$. Bloembergen, Purcell, and Pound (1948) have thoroughly dealt with the influence of motion upon the spin interaction and have shown that when the average period of the reorientation motions approaches the value $1/2\pi\delta\nu$, the narrowing process begins. A correlation frequency, ν_c, is introduced as a measure of the reorientation frequency. The motional narrowing is shown to be described by the following function:-

$$(\delta\nu)^2 = (\delta\nu)_o^2 \frac{2}{\pi} \tan^{-1} \frac{\delta\nu}{\nu_c} \qquad \ldots\ldots\ldots(3)$$

where $(\delta\nu)_o$ is the rigid lattice linewidth.

It is through the dependence of ν_c on temperature that the narrowing of the line is expressed as a function of temperature. If the molecular motion is thermally activated, ν_c can be expressed as

$$\nu_c = \nu_o e^{-E/RT}$$

where E is a measure of the activation energy of the reorientation.

The common procedure is to fit equation (3) to observed linewidth versus temperature curves in order to arrive at a value of the energy E. A comparable result can be obtained if the root second moment $\sqrt{(\Delta\nu)^2}$ is substituted for the linewidth.

The theories that have been presented in this section are by no means the most refined of those available to analyze motional narrowing. Considerably more detailed developments have appeared, based on these first fundamental approaches. However, it is believed that in the present work concerning the study of molecular motion in natrolite, the basic theory suffices to yield meaningful results.

CHAPTER II

Apparatus

The nuclear magnetic resonance spectrometer used in this work is of conventional design. The external field is provided by a Varian electromagnet with pole faces 12 inches in diameter and 3 inches apart. A current of up to two amperes is supplied to the high impedance windings from mercury vapour rectifiers. For field stabilization, the resonance signal from the F^{19} nuclei in a teflon cylinder is continually detected and degeneratively fed back to a bank of power triodes through which the magnet current passes, thereby automatically adjusting the current to stabilize the value of the applied field to 1 part in 250,000.

The oscillating detector is of the type described by Volkoff, Petch, and Smellie (1952). The spectrum is scanned by slowly varying the capacity in the oscillator tank circuit. This is done by means of a Haydon clock drive motor and reduction gears. The sweep rate used in this work was of the order of 50 c./s. A General Radio frequency meter type 620A and a Hallicrafters Model SX-62A communications receiver are used to measure the frequency of the oscillating detector with an accuracy of about 1500 c./s.

The external magnetic field is modulated by a 220 c./s. sine wave from a Hewlett-Packard 200AB audio oscillator which is amplified to provide a modulation amplitude of about 10^{-4} wb./m.^{2} The r.f. signal in the oscillating detector is thus modulated at 220 c./s., the modulation being proportional to the first derivative of the absorption curve. The r.f. signal is passed through a detector stage. The a.f. output is amplified in a narrow band amplifier tuned to 220 c./s. and then fed to a phase-sensitive detector. The d.c. output of the detector, which is proportional to the absorption derivative, is measured by a Varian G10 (100 mv.) recording millivoltmeter. Frequency markers are accurately placed on the recorder chart at intervals of a few kc./s.

Single crystal samples are oriented in the external magnetic field by a simple device. The rotation axis is a teflon shaft mounted in a heavy brass block which is clamped between the magnet pole pieces so that the rotation axis is perpendicular to the applied field. An accurately calibrated circular Vernier scale at one end of this shaft provides a measurement of the rotation angle ϕ with an accuracy of about six minutes of arc. At the other end of the shaft is mounted a Unicam single crystal goniometer system which holds the crystal at the center of the magnetic field and gives it two more degrees of freedom, enabling one to bring the desired crystal axis parallel to

the rotation axis. The sample and goniometer system are enclosed in a brass cup which serves two purposes: it affords the necessary r.f. shielding of the oscillator coil and it forms an enclosed chamber to facilitate heating or cooling of the sample in studies of the temperature dependence of the spectral pattern.

Powder samples are usually sealed in a soft glass tube and mounted directly to the teflon rotation shaft without the use of the goniometer. The r.f. coil consists of a few turns of bare silver wire cemented to the glass sample bottle.

The system for heating samples is fairly simple. Air from the low pressure tap in the laboratory is blown through a pyrex tube containing a nichrome heater element and then fed into the brass can surrounding the sample, from where it escapes via a small port. The temperature is controlled by a variable transformer which supplies the heater coil and by the tap which controls the rate of flow of the air. Temperatures up to 300°C. were easily reached and maintained to within 1 centigrade degree.

An even simpler system was used for cooling the samples. A small nichrome heater coil connected to a variable transformer was used to boil air from a large container of liquid air. This cold dry air was fed directly to the sample holder exactly as in the heating arrangement. Changing the boiling rate of the air by adjustment of the

variable transformer gave suitable control of the temperature. Temperatures as low as -120°C. were readily achieved and maintained to within 1 centigrade degree.

The temperature of the powder samples was measured by a copper-constantan thermocouple. One junction was located in the center of the powder while the reference junction was kept in a water bath of known temperature. By employing a Croydon Thermocouple Potentiometer one could determine the sample temperature with an accuracy of about 0.5° C.

CHAPTER III

Natrolite, a Fibrous Zeolite

The structure of the silicate minerals is based upon the SiO_4 tetrahedron in which the silicon ion is at the center of the tetrahedron and the oxygen ions form its four corners. A three-dimensional framework, which is formed when each tetrahedron shares all four corner oxygen atoms with other tetrahedra, characterizes several classes of silicate minerals, including the zeolites. Al^{+++} can be substituted for Si^{++++} because the interstitial position in an oxygen tetrahedron provides a site of suitable volume and co-ordination. The complete structure must satisfy all valencies and have no net charge. To neutralize the negative charge arising from the AlO_4- tetrahedra the crystal must contain a cation such as K^+, Na^+, Ca^{++}, or Ba^{++}, in the appropriate amount. The co-ordination required by such ions is not critical and they normally occupy relatively large spaces surrounded by eight or more oxygen atoms.

The zeolites resemble the feldspars, feldspathoids, and ultramarines in that the framework consists of AlO_4 and SiO_4 tetrahedra linked in such a way that the ratio (total no. of oxygen atoms)/(total Al + Si) = 2 ; but they have, as their name indicates, the distinguishing feature of being hydrated. More specifically, they are characterized by

reversible dehydration and cation exchange processes. The fibrous zeolites edingtonite, thomsonite, natrolite, scolecite, and mesolite are all built of the same chains of linked tetrahedra and differ only in the size of the unit cell, the type of linkage between silicate chains, and the position of the symmetry axes and planes which relate each chain to all the others.

The crystallographic data for natrolite is as follows:-

orthorhombic; space group Fdd2 - C_{2v}^{19}

a = 18.30 $\pm$ 0.01 A.

b = 18.63 $\pm$ 0.01 A.

c = 6.60 $\pm$ 0.02 A.

This data is after Meier (1960).

The chemical formula is $Na_2Al_2Si_3O_{10}.2H_2O$ with the fixed ratio Al/Si = 2/3. Eight of these formula units make up one unit cell. Natrolite which has formed in the normal habit appears as long needles parallel to the $\vec{c}$ axis. The colour is often white; the specific gravity is 2.25; and the hardness is greater than 5.

Chains of AlO_4 and SiO_4 tetrahedra extend without limit in the $\vec{c}$ direction. As seen in Fig. 4, the AlO_4 and SiO_4 tetrahedra occur in an ordered arrangement and each chain is joined to the others at its four corners in such a way as to make a strong silicate framework with large pores to accommodate the cations and water molecules. The wide clear channels parallel to the $\vec{c}$ axis are intercon-

Figure 4

(a) A diagram showing the hydrogen bonds (dashed lines) linking the water molecule to the AlO_4 and SiO_4 tetrahedra in natrolite.

(b) A projection of the natrolite structure on the (001) plane. The AlO_4 tetrahedra are shaded.

(After Meier)

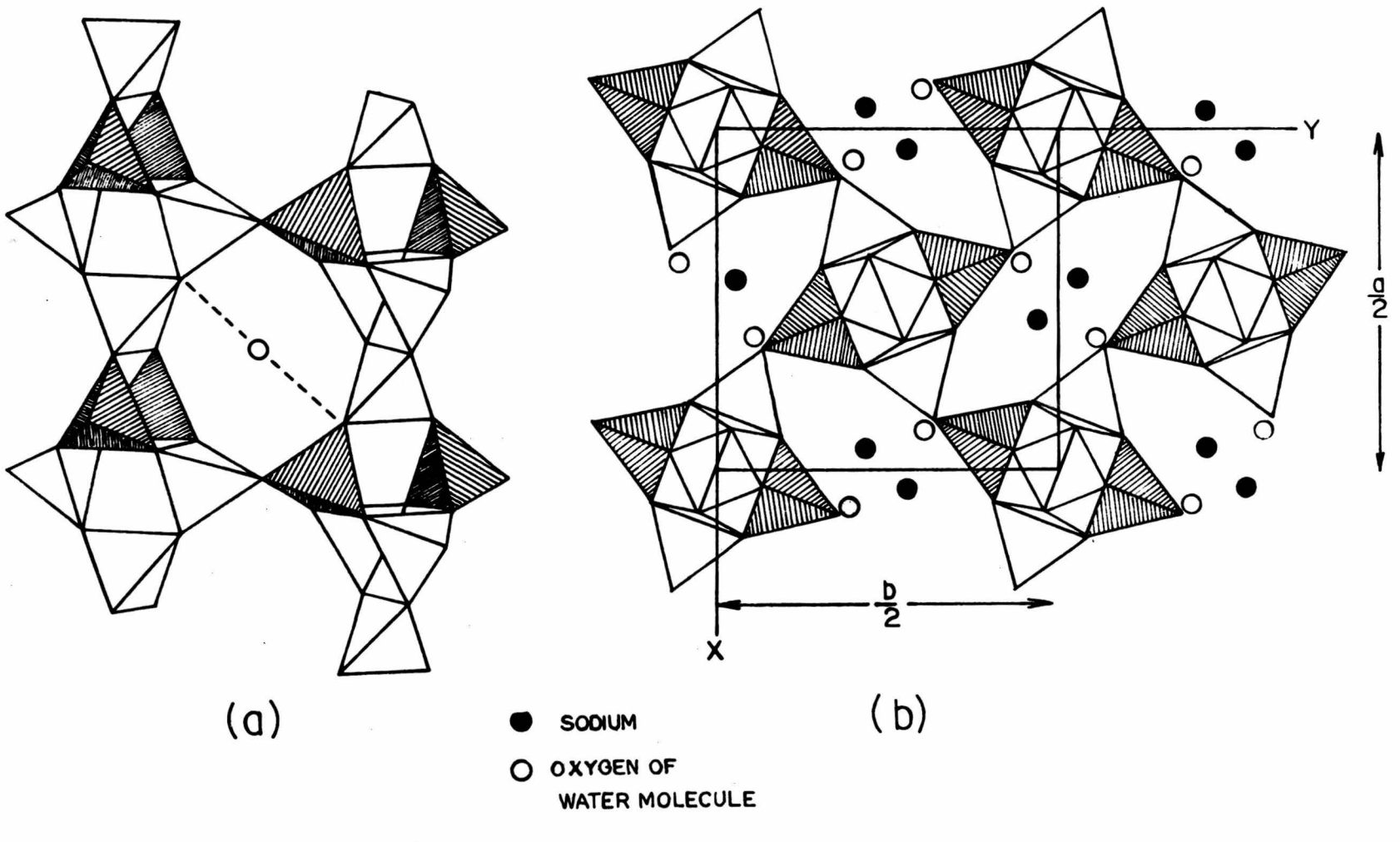
Y
X
b/2
a/2
(a)
(b)
SODIUM
OXYGEN OF
WATER MOLECULE

nected by smaller tortuous channels which further increase the porosity of the mineral.

In the several studies that have been made of the dehydration process in natrolite during the last hundred years, considerable difficulty has been met in arriving at the true nature of the process. Control of the water vapour pressure seems to be of some importance. The proper degree of dehydration for a given temperature is reached only after several hours of holding the sample at that temperature. Many workers have found that the water is more reluctant to leave the channels after each subsequent dehydration and rehydration. Measurements of the heat of hydration have been somewhat difficult to interpret owing to the serious shrinkage of the silicate framework as the water leaves the pores and the strong tendency for the natrolite to adsorb water on its surface. Nevertheless the general character of the isobaric dehydration curve has been established; for a water vapour pressure of 10 m.m. more than 90% of the dehydration occurs over a range of a very few degrees somewhere between 260° and 290° C. The mechanism of the absorption of small molecules in the pores of the zeolites has been likened to the simple operation of a sponge. Not every liquid or vapour can be absorbed; some molecules are too large to enter the channels. Yet one finds, for example, hydrogen, carbon dioxide, alcohol, hydrogen sulphide, air, iodine, mercury, sulphur, and ammonia in the long list of substances known to be readily absorbed by most zeolites.

However, the cations and water in the zeolites are not so independent of the silicate structure as might be suggested. In natrolite, at room temperature, the water molecules and sodium atoms occupy definite sites in an ordered arrangement. The bonding of the water to the SiO_4 tetrahedra is probably, as suggested by Meier, accomplished in the manner shown in Fig. 4a.

CHAPTER IV

Procedure and Results

IV. 1. Introduction

This chapter describes the procedure followed in the proton magnetic resonance study of natrolite, both in single crystal and powdered forms. An account is given of the measurements made and the information gained about the location and mobility of the waters of hydration.

IV. 2. Single Crystal Work

The first step in the investigation was a study of the proton spectrum for several orientations of the applied field with respect to the crystallographic $\vec{b}$ and $\vec{c}$ axes as the crystal was rotated about its $\vec{a}$ axis, this rotation axis being perpendicular to the field. The desired crystal orientation with respect to the field and the rotation axis was achieved by observing the quadrupole spectra of the Al^{27} and Na^{23} nuclei and making use of the coalescence of satellite signals from the symmetry-related Al and Na sites which occurred whenever the applied field was perpendicular to any of the three crystal axes. Complete knowledge of the orientational dependence of these quadrupole spectra as given by Petch and Pennington (1962) was invaluable in this alignment procedure.

Two broad proton lines were observed; their width was approximately 12 kc./s. The frequency separations ($\Delta\nu$) of the absorption peaks were measured for various values of the angle between the applied field and the $\vec{b}$ axis of the crystal. The results are given in Table I. A plot of $\Delta\nu$ versus Φ is given in Fig. 5. The origin of the rotation is chosen such that $\Phi = 0^{\circ}$ when B_o is parallel to the $\vec{b}$ axis of the crystal.

The unit cell of natrolite contains four non-identical water molecules so that for an arbitrary crystal orientation one would expect to observe four pairs of absorption peaks in the proton resonance spectrum. In the $\vec{a}$ rotation the applied magnetic field lies in the crystal mirror plane so that sites related by the mirror plane give identical results. Hence, only two pairs of absorption peaks would be expected to appear. However, it turned out that these peaks so nearly coincided that they could not be resolved because, as was later determined, the projections of the two p-p lines on the plane perpendicular to the rotation axis are approximately at right angles and the angle ($\frac{\pi}{2} - \delta$) between the p-p lines and the rotation axis is within a few degrees of $54^{\circ}44'$.* In fact, further work has shown that no resolution of the separate Pake curves is possible for rotations about any of

---

* $54^{\circ}44'$ is $\sin^{-1}\sqrt{2/3}$. When $\frac{\pi}{2} - \delta = 54^{\circ}44'$ the positive and negative extrema of $\Delta\nu$ are equal in magnitude.

TABLE I

Observed value of frequency separation of the proton resonance lines for a rotation of a single crystal of natrolite about its $\vec{a}$ axis.

Rotation angle, ϕ, degrees	Independent observations of line separation, kc./s.				
30	34.4	35.0	36.8	33.4	35.0
	34.7	35.0	34.5	33.9	34.9
	33.7	34.2	34.8	34.1	35.1
	34.3	34.4	34.3	34.3	
40	39.8				
41	40.8				
42	40.5	40.0			
43	40.1	40.6			
44	40.2	40.7			
45	40.8	40.5	40.8	40.6	40.6
	39.7	40.7	39.9		

Figure 5

The frequency separation ($\Delta\nu$) of the proton lines plotted against the rotation angle Φ for rotation about the $\vec{a}$ axis of the crystal. The black dots represent the average of the observed values (given in Table I) for each value of Φ. The solid line is a plot of 40.2 sin 2 Φ kc./s.

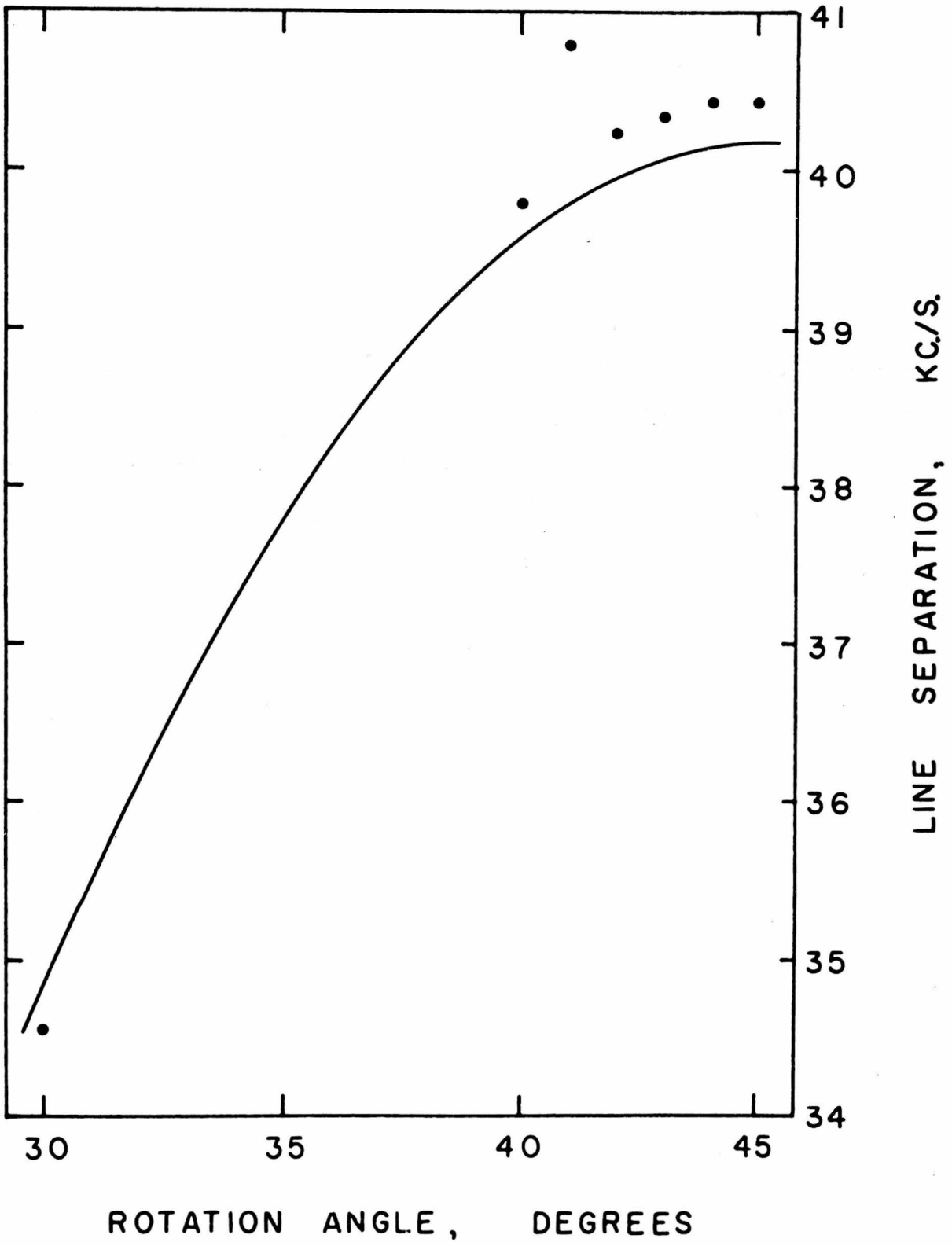
41
40
39
38
37
36
35
34
30
35
40
45
LINE SEPARATION, KC./S.
ROTATION ANGLE, DEGREES

the three crystal axes because of the near coincidence of the frequency versus angle plots which arises from the conditions outlined above, thus making it impossible to employ the usual Pake method of determining the interproton distance and the orientation of the p-p line.

Fortunately it was possible to make a direct measurement of r, the interproton distance. The p-p lines are oriented such that when the field is made parallel to any one of them thereby producing a large separation between its pair of lines, the other three p-p lines make angles θ with the field such that none of the six lines are located far enough from the free proton frequency ν_0 to overlap the lines in the pair from the p-p lines parallel to B_0. The crystal orientation was adjusted so as to obtain the maximum possible separation of these two lines. In this situation we have θ of equation (1) equal to zero. The maximum value of $\Delta\nu$ obtained was 85.63 kc./s. Setting this equal to $3\mu_z^2 \mu_0 / \pi h r^3$ we find that r = 1.6144 Angstroms.

To obtain the orientation of the p-p directions, a rotation was done about an axis in the crystal lying in the $\vec{a}$-$\vec{b}$ plane and making an angle of $33^{\circ}00' \pm 06'$ with the $\vec{a}$ axis. This rotation was chosen as it allows one of the pairs of lines to be well resolved from the other three pairs for a sufficiently large portion of the rotation to permit one to locate the appropriate p-p direction. The observed frequency dependence of the signals upon the rotation angle Φ is given

in Table II and plotted in Fig. 6. Φ was chosen to be zero for the position where the field lay in the $\vec{a}$-$\vec{b}$ plane. The positive extremum of $\Delta\nu$ as given by equation (2) and the point where $\Delta\nu = 0$ were directly observed. Using the value of r determined above, equation (2) was fitted by the method of least squares to the pair of lines corresponding to the water molecules whose p-p lines made the smallest angle with the plane perpendicular to the rotation axis. The values obtained for the parameters are:-

$$\delta = 13.6^{\circ} \pm 0.5^{\circ}$$
$$\Phi_{o} = 36.9^{\circ} \pm 0.2^{\circ}$$

By spherical trigonometry the direction cosines of one of the p-p vectors with respect to the crystallographic axes are found to be:-

$$\alpha = .621 \pm .008$$
$$\beta = .523 \pm .005$$
$$\gamma = .584 \pm .003$$

The directions of the three other p-p vectors are obtained by the operation of the symmetry elements of the crystal.

On the basis of this information the observed line separation for the rotation about the $\vec{a}$ axis can now be interpreted. While this rotation does not aid in the determination of the location of the protons, it does serve

TABLE II

Observed values of frequency separation of a pair of proton resonance lines for a rotation of a single crystal of natrolite about an axis lying in the $\hat{a}$-$\vec{b}$ plane and making an angle of 33°00' with the $\hat{a}$ axis

Rotation angle, Φ, degrees	Independent observations of line separation kc./s.		
-16°42'	0.0		
15	61.5	60.3	60.2
16	63.9		
17	64.6		
18	65.8		
19	67.4		
20	68.2		
25	73.5	74.0	
30	77.5	76.9	
35	78.4		
40	78.1		
45	76.9	77.0	
50	72.8	71.6	
55	65.9		
60	59.0		

Figure 6

The angular dependence of the frequency separation of the two resolvable lines for a rotation of the crystal about an axis lying in the $\vec{a}$-$\vec{b}$ plane and making an angle of $33^{\circ}00'$ with the $\vec{a}$ axis. The black dots represent the average of the observed values (given in Table II) for each value of Φ. The solid line is a plot of

$$\frac{85.63}{2}\left[3\cos^2(\Phi - 36.9^{\circ})\cos^2 13.6^{\circ} - 1\right] \text{ kc./s.}$$

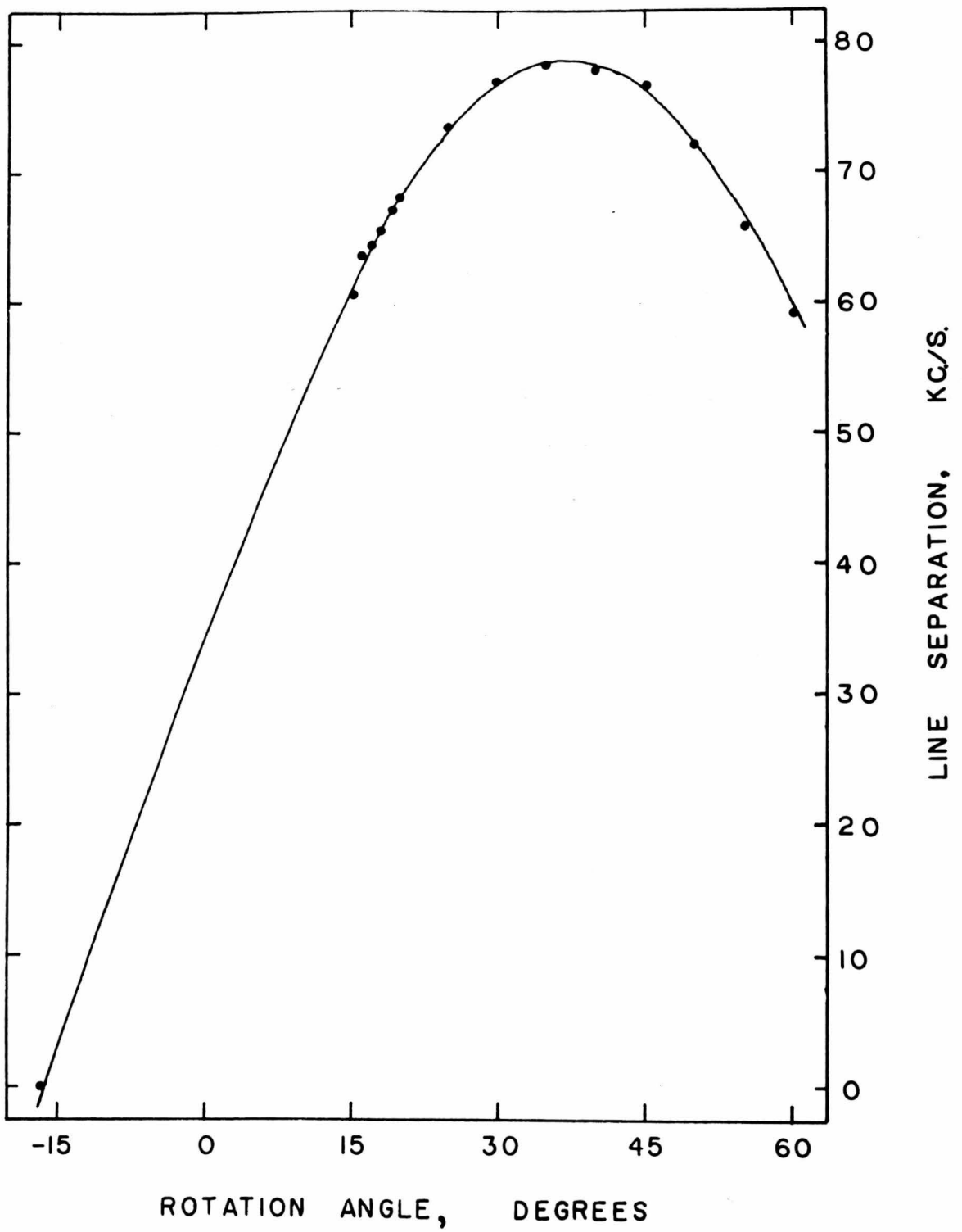
80
70
60
50
40
30
20
10
0
LINE SEPARATION, KC/S.
-15
0
15
30
45
60
ROTATION ANGLE, DEGREES

Figure 7

Proton spectrum of a single crystal of natrolite showing the resolution of the two outermost lines for the value $\Phi = 35^{\circ}$ in Fig. 6. The markers are placed at frequency intervals of 20 kc./s.

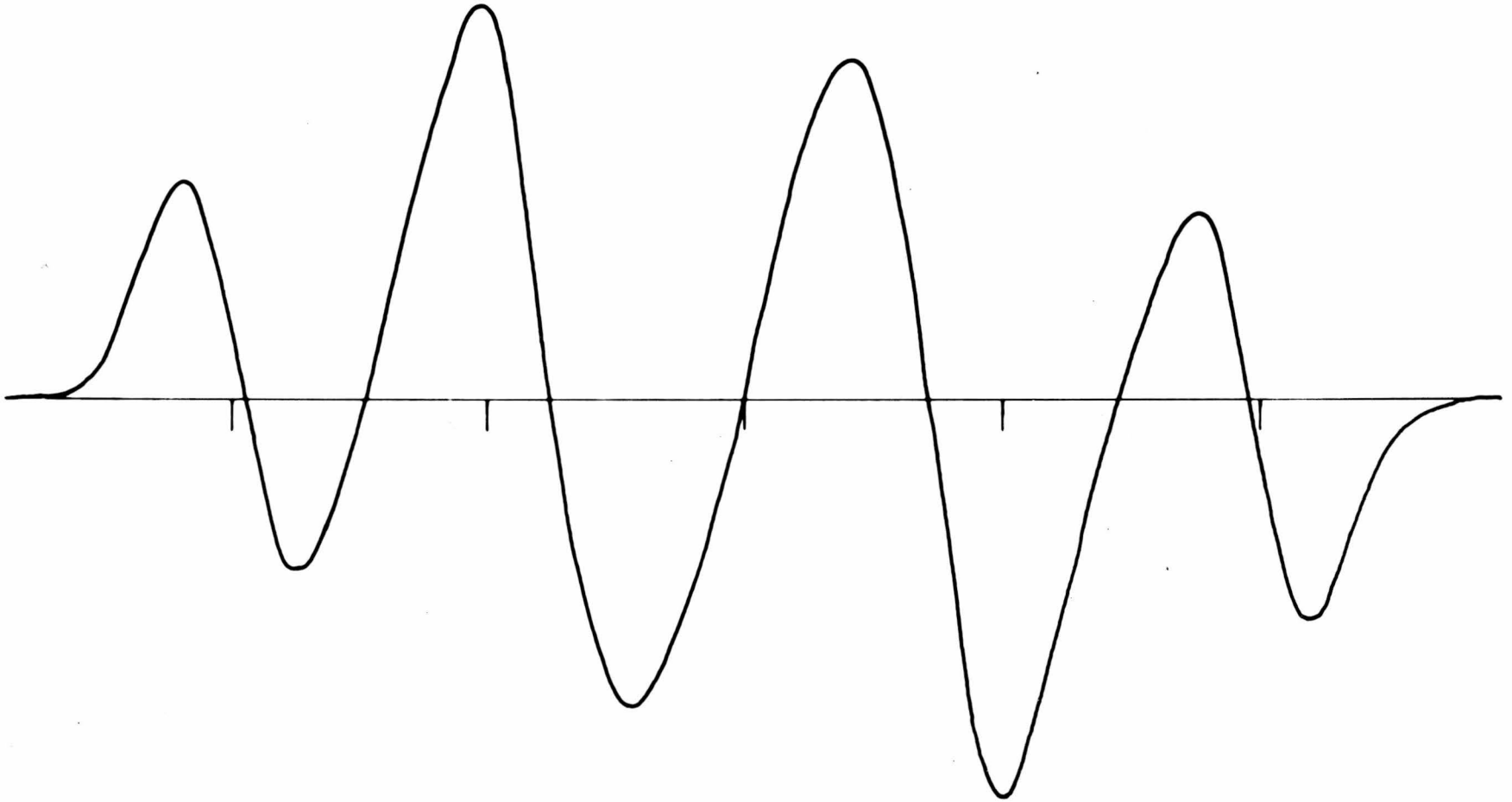

as a useful check that the behaviour of the spectrum as the field orientation changes can be adequately described by Pake's theory for rigid proton pairs. The observed line separation follows a curve which is the average of the two unresolved curves giving the separation of the pairs for this rotation. The two Pake curves have the same values of r and δ while the values of Φ_o are equal in magnitude but opposite in sign. For all portions of the rotation except those for which the field lies within about five degrees of the $\vec{b}$ or $\vec{c}$ axes, the two values of $\Delta\nu$ as given by equation (2) are approximately equal in magnitude but opposite in sign. Thus except for Φ near 0, 90, 180, or 270 degrees the observed line pair separation is expected to follow a curve obtained by taking half the difference between two curves of the form of equation (2), one having a phase angle Φ_o and the other a phase angle $-\Phi_o$. The resultant equation is

$$\Delta\nu = \frac{9}{4} \frac{\mu_z^2 \mu_o}{\pi h r^3} \cos^2\delta \sin 2\Phi_o \sin 2\Phi$$

The mirror symmetry of the crystal and the symmetry of the $\sin 2\Phi$ function make it unnecessary to consider values of Φ greater than 45^o. A least squares fitting of this equation to the observations for this rotation yields the following result:-

$$\frac{9}{4} \frac{\mu_z^2 \mu_o}{\pi h r^3} \cos^2\delta \sin 2\Phi_o = 40.2 \pm 0.1 \text{ kc./s.}$$

where r, δ , and Φ_0 are the unknown parameters of the curve. The curve predicted on the basis of the previously given values of the direction cosines of the p-p lines is the following:-

$$\Delta\nu = 39.2 \sin 2\Phi \quad kc./s.$$

with which the observations agree well considering the error involved in measuring the separation of the broad distorted lines encountered in the $\vec{a}$ rotation.

IV. 3. Proton Resonance in Natrolite Powder

The proton resonance spectrum of natrolite was studied with several powder samples and at many different temperatures. Absorption derivative curves obtained at several temperatures are shown in Fig. 8. At room temperature the resonance is typical of rigid pairs of protons in a powder. As the temperature increases there is a very gradual narrowing of the line and consequential decrease in second moment. A narrow resonance of about 6 kc./s. width begins to appear in the center of the pattern at a temperature which was found to depend strongly on the past history of the sample, the amount of water adsorbed on its surface, and other factors. Although the linewidth and second moment values were not closely reproducible in the temperature range just above room temperature, the width of the resonance was always found to decrease suddenly as the temperature rose above

Figure 8

The observed proton spectra of powdered natrolite at several temperatures. The frequency markers on the horizontal scale are at intervals of 20 kc./s.

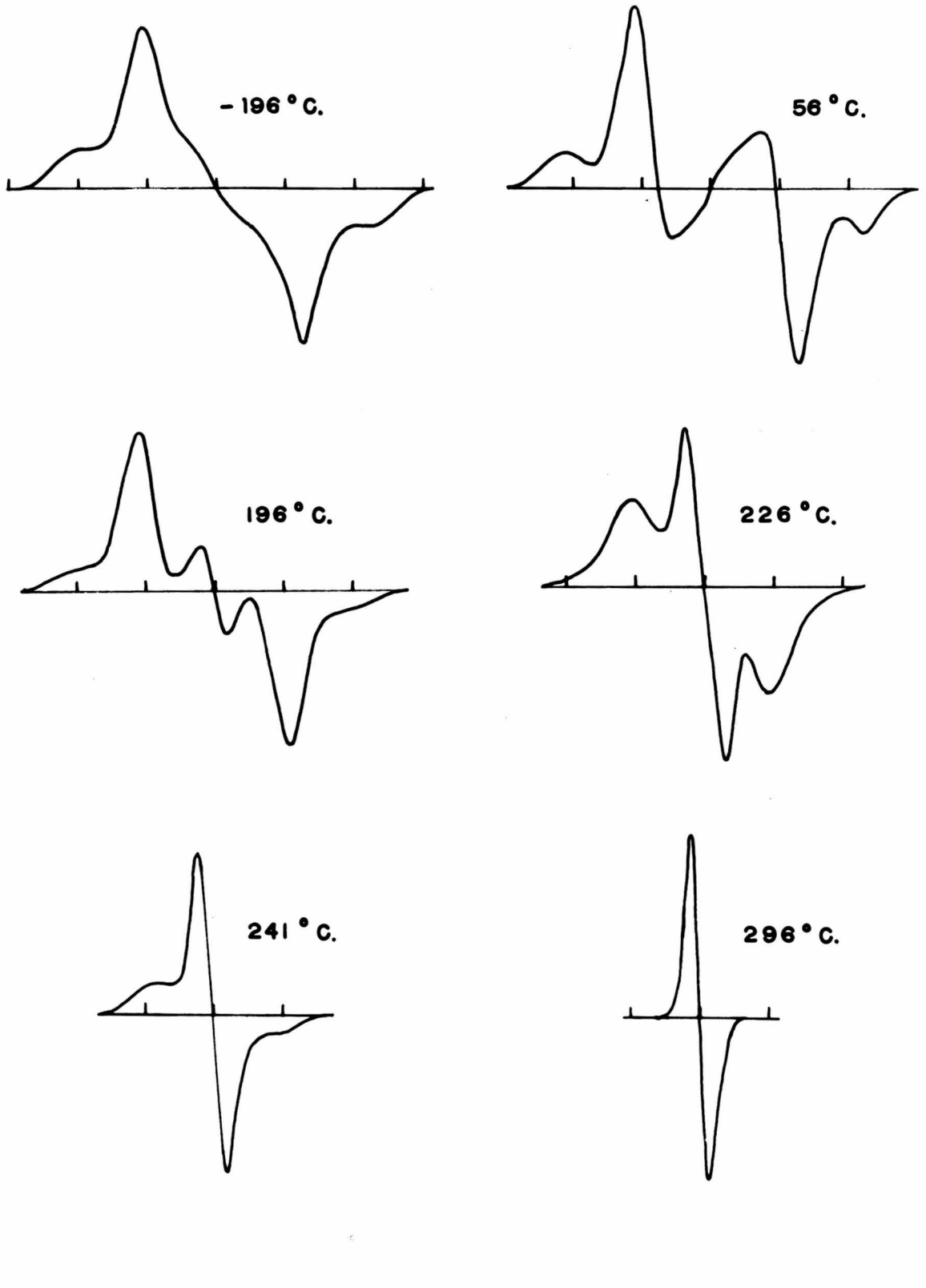
-196 °C.
56 °C.
196 °C.
226 °C.
241 °C.
296 °C.

220° C. Rapid growth of the narrow central peak was simultaneous with the rapid decrease in the intensity and separation of the outer peaks.

In order to determine the activation energy for motion of the water molecules, the second moment and the linewidth data are plotted against temperature in Figs. 9 and 10. Up to about 230° C. the linewidth was taken as the frequency separation between the maximum and the minimum of the absorption derivative curve. Above this temperature the linewidth, taken as the frequency separation between these same outer peaks, became increasingly difficult to measure accurately as the outer peaks fell in strength and merged with the wings of the signal growing in the center. In Figs. 9 and 10 the dots represent the observed values while the solid lines are plots of equation (3) with values 9 and 12 kcal./mole for the activation energy in Fig.9 and values 10 and 14 kcal./mole in Fig.10.

Figure 9

The temperature dependence of the linewidth of the proton spectrum of powdered natrolite. The black dots denote the observed values. Solid curves (a) and (b) are plots obtained using equation (3) and values for the activation energy of 12 and 9 kcal./mole respectively.

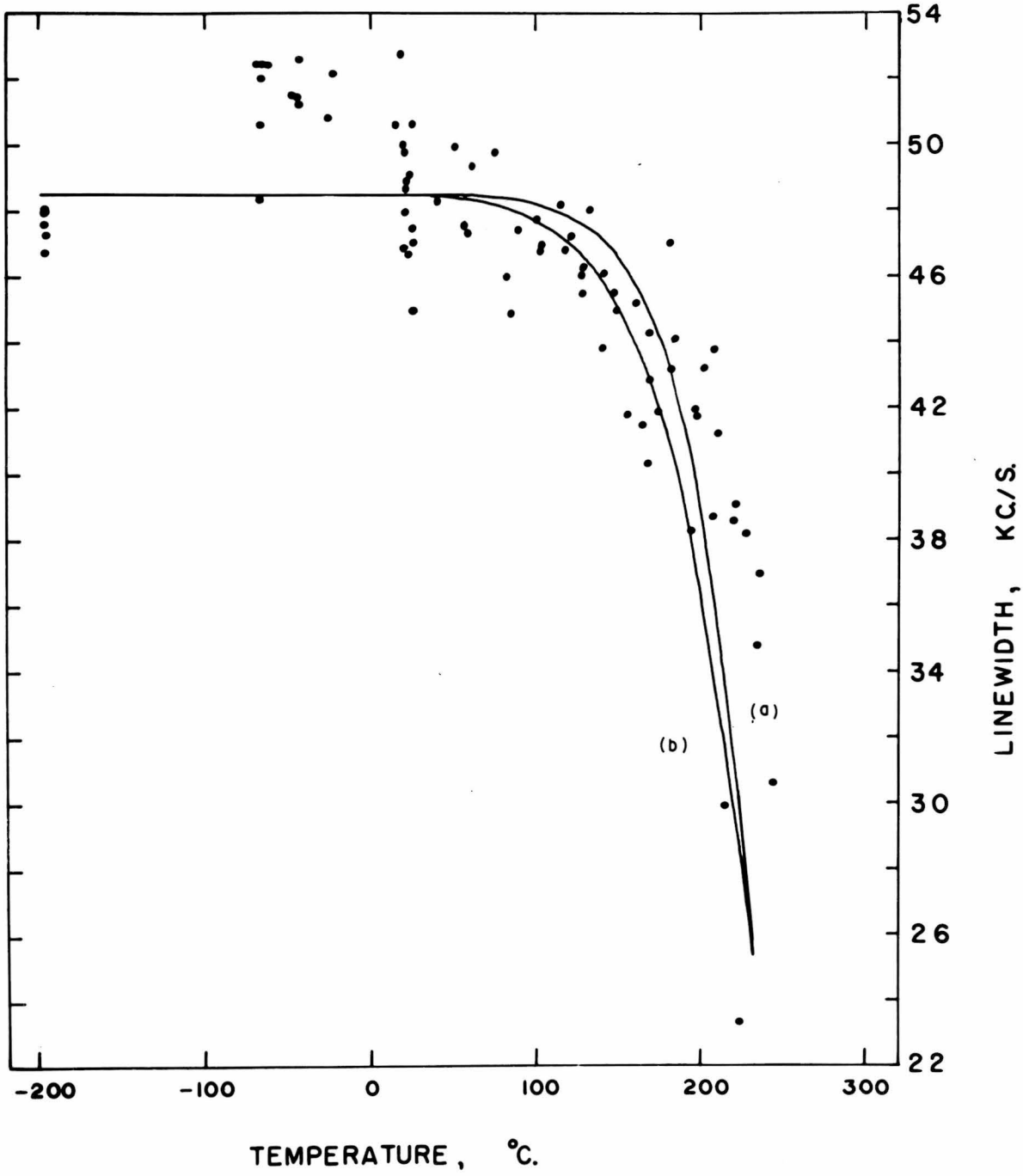
54
50
46
42
38
34
30
26
22
LINEWIDTH, KC/S.
(a)
(b)
-200
-100
0
100
200
300
TEMPERATURE, °C.

Figure 10

The temperature dependence of the second moment of the proton spectrum of powdered natrolite. The black dots denote the observed values. Solid curves (a) and (b) are plots obtained using equation (3) (with $(\delta\nu)^2$ replaced by the second moment) and values for the activation energy of 14 and 10 kcal./mole respectively.

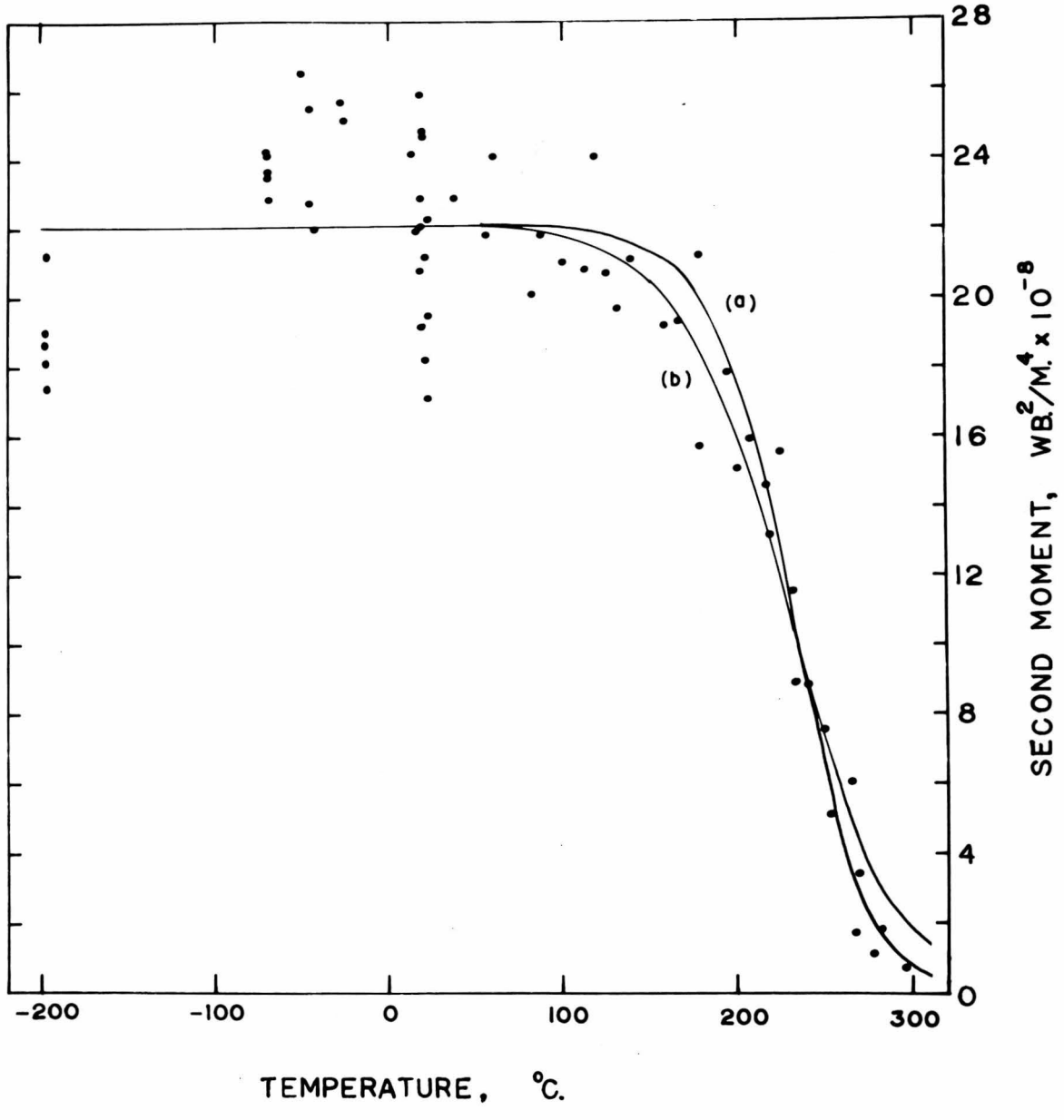
28
24
20
16
12
8
4
0
SECOND MOMENT, WB.²/M.⁴ x 10⁻⁸
(a)
(b)
-200
-100
0
100
200
300
TEMPERATURE, °C.

CHAPTER V

Discussion

V. 1. Single Crystal Work

The appearance of pairs of lines in the spectra of the single crystal sample and the observed orientational dependence of their separation confirm the belief that the water molecules in natrolite have only four permissible orientations with respect to the crystal axes, these four orientations being related to each other by the mirror planes of the structure.

The value given for r, the interproton distance, has a standard deviation of 0.0006 A. derived from the statistics of the plots made of $\Delta\nu$ versus field orientation in the neighbourhood of maximum $\Delta\nu$. However, the method used to measure line separations would allow a systematic error having a maximum value of 0.8 kc./s. A value of $\pm$ 0.005 A. is the corresponding maximum possible error in r. For comparison, values of the interproton distance in other hydrates are listed in Table III. An assumption that the water molecule forms an isosceles triangle with an H - O - H angle of 108°, a typical value, results in an O - H distance of 1.00 A. which compares favourably with the values listed in Table IV.

TABLE III

Interproton distances in natrolite compared with values obtained in other hydrates

Compound	Interproton distance, A.	Method used	Reference
$Na_2Al_2Si_3O_{10}.2H_2O$	1.614 ± .005	proton resonance	This Work
	1.56 ± .04	neutron diffraction	Torrie (1962)
$CaSO_4.2H_2O$	1.58 ± .02	proton resonance	Pake (1948)
$CuCl_2.2H_2O$	1.60	proton resonance	Itoh et al. (1953)
$Ba(ClO_3)_2.2H_2O$	1.61 ± .01	proton resonance	Silvidi and McGrath (1961)
$K_2CuCl_4.H_2O$	1.62	proton resonance	Itoh et al. (1953)
$BaCl_2.2H_2O$	1.58 ± .02	proton resonance	Silvidi and McGrath (1960)

TABLE IV

O - H distance in natrolite compared with that in other substances

Compound	O - H distance, A.	Method used	Reference
$Na_2Al_2Si_3O_{10}.2H_2O$	1.00	proton resonance	This work
	0.94 and 0.98	neutron diffraction	Torrie (1962)
H_2O (steam)	0.96		
H_2O (ice)	1.01		
$Na_2CO_3.NaHCO_3.2H_2O$	1.01 $\pm$ .02	neutron diffraction	Bacon and Curry (1956)
$CaSO_4.2H_2O$	0.99	neutron diffraction	Atoji and Rundle (1958)

The direction cosines of the p-p vectors compare well with the following values calculated from the co-ordinates of the protons in the unit cell as measured by Torrie (1962) using neutron diffraction:-

This work	Neutron diffraction
α = .621 $\pm$ .008	α = .586 $\pm$ .020
β = .523 $\pm$ .005	β = .526 $\pm$ .019
γ = .584 $\pm$ .003	γ = .617 $\pm$ .028

The angle between the p-p line direction calculated from the neutron diffraction results and the p-p direction obtained in this work is 2.8 degrees.

V. 2. Powder Work

The large width of the room temperature proton resonance obtained in this work, about 50 kc./s., is the value expected from proton pairs with a separation of 1.6 A. provided there is no motion of the molecule. It is clear then that at room temperature the water of hydration in natrolite has little mobility, as was reported by Ducros (1960). The observed narrowing of the signal indicates that the water molecules undergo rapid and extensive re-orientation with rising temperature. The linewidth versus temperature plot strongly suggests that this reorientation causes the linewidth to fall to zero rather than to some finite value. It is not likely then that the water molecules rotate about one fixed axis but rather that they execute a

more general motion at their lattice sites. The appearance of a very narrow resonance line at high temperatures is probably associated with water molecules which have become unbound in the lattice and saltate from one water site to another in the channels of the crystals, remaining free for long enough periods of time to experience an averaging out of dipolar interactions. From the increasingly rapid growth of this component of the absorption as the temperature rises it can be seen that all of the water eventually becomes unbound, as it must do considering the impending dehydration of the crystals at a temperature not far above 260° C.

The determination of an activation energy for the reorientation of the water molecules in natrolite is a somewhat uncertain matter when a plot of linewidth versus temperature is employed. The major difficulty in this work is the problem of defining the linewidth and observing a large decrease in it with rising temperature. The linewidth was taken to be the separation of the derivative peaks of that portion of the resonance characteristic of bound pairs of protons, as stated in the previous chapter. At temperatures below 200° C. the linewidth of each recorded derivative could be measured to within about 1 kc./s. However, above 200° C. the narrow signal in the center of the resonance was strong enough to mask the signal whose width was being taken as a measure of the linewidth for purposes

of obtaining a value of the activation energy. In such cases it was often difficult to determine the linewidth to within 2 or 3 kc./s. Furthermore, the great variation of linewidth as observation of the resonances was repeated at a given temperature causes the slope of the linewidth verses temperature curve to be less definite. In addition the assumption was made that for temperatures above 300° C. the linewidth approached zero rather than a finite value.

The behaviour of the resonance line is more completely and less ambiguously described by the variation of second moment with temperature. For all values of temperature the second moment of a recording of the spectrum could usually be determined to within 1×10^{-8} wb.^{2}/m.^{4} , although the variations for different recordings of the spectrum at a given temperature were as considerable as in the case of linewidth measurement. Modification of equation (3) to describe the change in second moment depends on there being a fixed ratio between the second moment and the square of the linewidth as the line experiences motional narrowing. In the case of natrolite, this ratio is not very constant thus detracting from the significance of the value of activation energy obtained from second moment measurements.

The value of activation energy obtained for reorientation of the water molecules in the channels is not expected to differ greatly from the activation energy for expulsion of the molecules from the channels in the form of liquid water.

Hey (1932) gives a value of 12.3 kcal./mole for the mean heat of hydration of natrolite in the reaction with liquid water, which value falls within the range suggested by this work for molecular reorientation.

BIBLIOGRAPHY

Atoji, M. and Rundle, R.E.

- J. Chem. Phys. 29: 1306, 1958.

Bacon, G.E. and Curry, N.A.

- Acta Cryst. 9: 82, 1956.

Bloch, F., Hansen, W.W. and Packard, M.

- Phys. Rev. 70: 474, 1946.

Bloembergen, N., Purcell, E.M. and Pound, R.V.

- Phys. Rev. 73: 679, 1948.

Ducros, P. - Bull. Soc. franc. Miner. Crist. 83: 85, 1960.

Hey, M.H. - Mineralogical Magazine 23: 243, 1932.

Itoh, J., Kusaka, R., Yamagata, Y., Kiriyamo, R. and Ibamoto, H.

- Physica 19: 415, 1953.

Meier, W.M.

- Z. Kristallogr. 113: 430, 1960.

Pake, G.E.

- J. Chem. Phys. 16: 327, 1948.

Petch, H.E. and Pennington, K.S.

- J. Chem. Phys. 36: 1216, 1962.

Purcell, E.M., Torrey, H.C. and Pound, R.V.

- Phys. Rev. 69: 37, 1946.

Rabi, I.I., Millman, S., Kusch, P. and Zacharias, J.R.

- Phys. Rev. 55: 526, 1939.

Silvidi, A.A. and McGrath, J.W.

- J. Chem. Phys. 32: 924, 1960.
  J. Chem. Phys. 34: 322, 1961.

Torrie, B.H.

- Ph.D. Thesis, McMaster University, Hamilton, Ontario, 1962.

Van Vleck, J.H.

- Phys. Rev. 74: 1168, 1948

Volkoff, G.M., Petch, H.E., and Smellie, D.W.L.

- Can. J. Phys. 30: 270, 1952.